environmental microbiology

Environmental Microbiology (2014) **16**(9), 2815–2830 doi:10.1111/1462-2920.12254

Distinct dissolved organic matter sources induce rapid transcriptional responses in coexisting populations of *Prochlorococcus*, *Pelagibacter* and the OM60 clade

Adrian K. Sharma,[1,6†] Jamie W. Becker,[2,6†] Elizabeth A. Ottesen,[1,3,6] Jessica A. Bryant,[1,6] Solange Duhamel,[2,4,6] David M. Karl,[5,6] Otto X. Cordero,[1] Daniel J. Repeta[2,6] and Edward F. DeLong[1,6*]

[1]*Departments of Civil and Environmental Engineering and Biological Engineering, Massachusetts Institute of Technology, Cambridge, MA 02139, USA.*
[2]*Department of Marine Chemistry and Geochemistry, Woods Hole Oceanographic Institution, Woods Hole, MA 02543, USA.*
[3]*Department of Microbiology, University of Georgia, Athens, GA 30602, USA.*
[4]*Lamont Doherty Earth Observatory, Columbia University, Palisades, NY 10964, USA.*
[5]*Department of Oceanography, School of Ocean and Earth Science and Technology (SOEST), University of Hawaii, Honolulu, HI 96822, USA.*
[6]*Center for Microbial Oceanography: Research and Education (C-MORE), 1950 East-West Road, Honolulu, HI 96822, USA.*

Summary

A considerable fraction of the Earth's organic carbon exists in dissolved form in seawater. To investigate the roles of planktonic marine microbes in the biogeochemical cycling of this dissolved organic matter (DOM), we performed controlled seawater incubation experiments and followed the responses of an oligotrophic surface water microbial assemblage to perturbations with DOM derived from an axenic culture of *Prochlorococcus*, or high-molecular weight DOM concentrated from nearby surface waters. The rapid transcriptional responses of both *Prochlorococcus* and *Pelagibacter* populations suggested the utilization of organic nitrogen compounds common to both DOM treatments. Along with these responses, both populations demonstrated decreases in gene transcripts associated with nitrogen stress, including those involved in ammonium acquisition. In contrast, responses from low abundance organisms of the NOR5/OM60 gammaproteobacteria were observed later in the experiment, and included elevated levels of gene transcripts associated with polysaccharide uptake and oxidation. In total, these results suggest that numerically dominant oligotrophic microbes rapidly acquire nitrogen from commonly available organic sources, and also point to an important role for carbohydrates found within the DOM pool for sustaining the less abundant microorganisms in these oligotrophic systems.

Received 17 April, 2013; revised 26 July, 2013; accepted 15 August, 2013. *For correspondence. E-mail delong@mit.edu; Tel. (+1) 617 253 5271; Fax (+1) 617 253 2679. †These authors contributed equally to this work.

Introduction

Nearly one half of global primary production occurs in the ocean (Field *et al.*, 1998) where a diverse group of phytoplankton fix carbon and nutrients into particulate organic matter (Azam, 1998). Exudation of metabolic waste products, viral lysis and predation all release a portion of microbial production into the water column as dissolved organic matter (DOM), a complex mixture of biochemicals of varying biological availability (lability) (Carlson, 2002) that changes in time and space (Aluwihare *et al.*, 1999; Mopper *et al.*, 2007; Kujawinski *et al.*, 2009). DOM supports secondary production and microbial respiration (del Giorgio and Duarte, 2002; Hansell *et al.*, 2009), with heterotrophic and mixotrophic picoplankton representing the main consumers. Understanding how picoplankton interact with this dynamic DOM reservoir is complicated by the inherent phylogenetic and population diversity of microbial communities, the complexities of their collective metabolic properties and interactions, and by our ability to measure microbial assemblage activities and responses on appropriate temporal and spatial scales. For these reasons, characterizing and quantifying microbial DOM cycling in the sea is a significant challenge.

Several recent studies using experimental incubations of seawater or microcosm perturbations have explored the consumption of phytoplankton-derived isotopically labelled DOM sources by examining uptake patterns and changes in community composition among diverse taxonomic groups (Nelson and Carlson, 2012; Sarmento and Gasol, 2012). These studies indicate that organisms with

different taxonomic affiliations and varying ecological growth strategies exhibit preferences in both the phytoplankton-derived origin and compositional properties of DOM. Other recent studies have combined meta-omics approaches with temporal field observations or experimental microcosm perturbations in neritic systems to gain insight into taxon-specific microbial responses to changes in naturally derived sources of DOM (Poretsky *et al*., 2010; Rinta-Kanto *et al*., 2012; Teeling *et al*., 2012; Landa *et al*., 2013). These studies highlight patterns of taxon-specific resource partitioning of DOM, community strategies for energy scavenging under carbon limitation and temporal successions of microbial populations in response to dynamic changes in natural DOM concentrations during a natural phytoplankton bloom. This previous work also demonstrates the utility of pairing DOM uptake experiments with meta-omics methodologies as a means of uncovering microbial taxa and metabolic strategies involved in marine DOM consumption.

The details of the functional and metabolic roles of specific microbial taxa in DOM degradation still remain largely unknown. Community response dynamics to DOM perturbations across short time scales are poorly understood, as most methods lack the necessary sensitivity to track transient responses. Such resolution would provide insight into the complex response mechanisms of microbial communities that result from both ecological variables and DOM resource partitioning. Here, we report a microcosm-based DOM perturbation experiment in an oligotrophic region of the ocean focused on measuring rapid temporal response dynamics over a 36 h period and the functional roles of oligotrophic taxa like *Prochlorococcus* and *Pelagibacter* that are ubiquitous in the open ocean (Lauro *et al*., 2009; Yooseph *et al*., 2010; Nelson and Carlson, 2012). Our microcosm perturbations involved the addition of natural sources of DOM to seawater collected from within the surface mixed layer (35 m) and placed in a temperature and light-controlled shipboard incubator. Incubations were conducted at Station ALOHA in the North Pacific Subtropical Gyre (NPSG), a region where the infrequency of deep-water mixing events results in low inorganic nutrient concentrations and limitation of primary production (Karl and Lukas, 1996; Karl *et al*., 2008). To study microbial communities under extreme oligotrophic conditions, perturbation experiments were conducted in late spring, a time of the year when the water column at Station ALOHA is highly stratified (Karl *et al*., 2012) and inorganic nutrient levels are frequently the most depleted (see Supporting Information Fig. S1).

To study differences in utilization of DOM from different sources, we examined the response of a single surface water microbial assemblage to perturbation with two distinct DOM types, comparing temporal observations from both treatments to a control microcosm. To examine breakdown of compounds in the standing DOM pool, we concentrated naturally occurring high-molecular weight dissolved organic matter (HMWDOM) on site from Station ALOHA surface seawater using an approach similar to that of McCarren and colleagues (2010). This size-fractionated DOM pool is considered to be 'semi-labile', rich in polysaccharides (Aluwihare *et al*., 2005) and other high-molecular weight compounds that might be preferred by specialist copiotrophic taxa (McCarren *et al*., 2010). In order to examine breakdown of newly produced 'labile' DOM, a second DOM source was prepared by concentrating the hydrophobic fraction of exudate from an axenic culture of *Prochlorococcus* strain MIT9313 (ProDOM). *Prochlorococcus* is the dominant photoautotroph in nutrient poor ocean gyres, and heterotrophic taxa in these regions are likely adapted to utilizing substrates derived from their photosynthate (Partensky *et al*., 1999; Bertlisson *et al*., 2005). The use of hydrophobic exudate material permitted direct chemical analysis of the treatment DOM by mass spectrometry, thus providing data on the nature of metabolites present and their size distribution.

We monitored microbial community responses to DOM amendments using a variety of methods and compared these observations to a control microcosm. Flow cytometry was used to track cell growth over a 36 h period, and β-glucosidase exoenzyme activity was determined from selected time points to assess polysaccharide utilization. Both metagenomic and metatranscriptomic data were obtained before perturbation from the 35 m seawater used for our microcosm experiment, as well as at 36 h after amendment. Combined with metatranscriptomic data from the intervening 2, 12 and 27 h time points, this experiment generated a detailed look at short-term temporal and functional responses of different microbial taxa to changes in ambient DOM quantity and quality.

Results

Microbial community growth and exoenzyme activity

The HMWDOM amendment increased concentrations of both dissolved organic carbon (DOC) and dissolved organic nitrogen (DON) by approximately 140%, while the ProDOM amendment increased DOC and DON by only 7% (Fig. 1A). DOC concentrations with standard deviation (SD) derived from triplicate measurements were 191 μM C (SD 0.35) for HMWDOM and 85.5 μM C (SD 0.35) for ProDOM, approximately 2.4× and 1.1× the ambient value of 79.9 μM C (SD 0.39) in the control microcosm. Both amendments increased DOC and DON concentrations in a manner that was proportional to the ratio of DOC : DON in the control. Despite these substantial differences in substrate quantity, both treatments induced similar patterns in growth relative to the control (Fig. 1B and C),

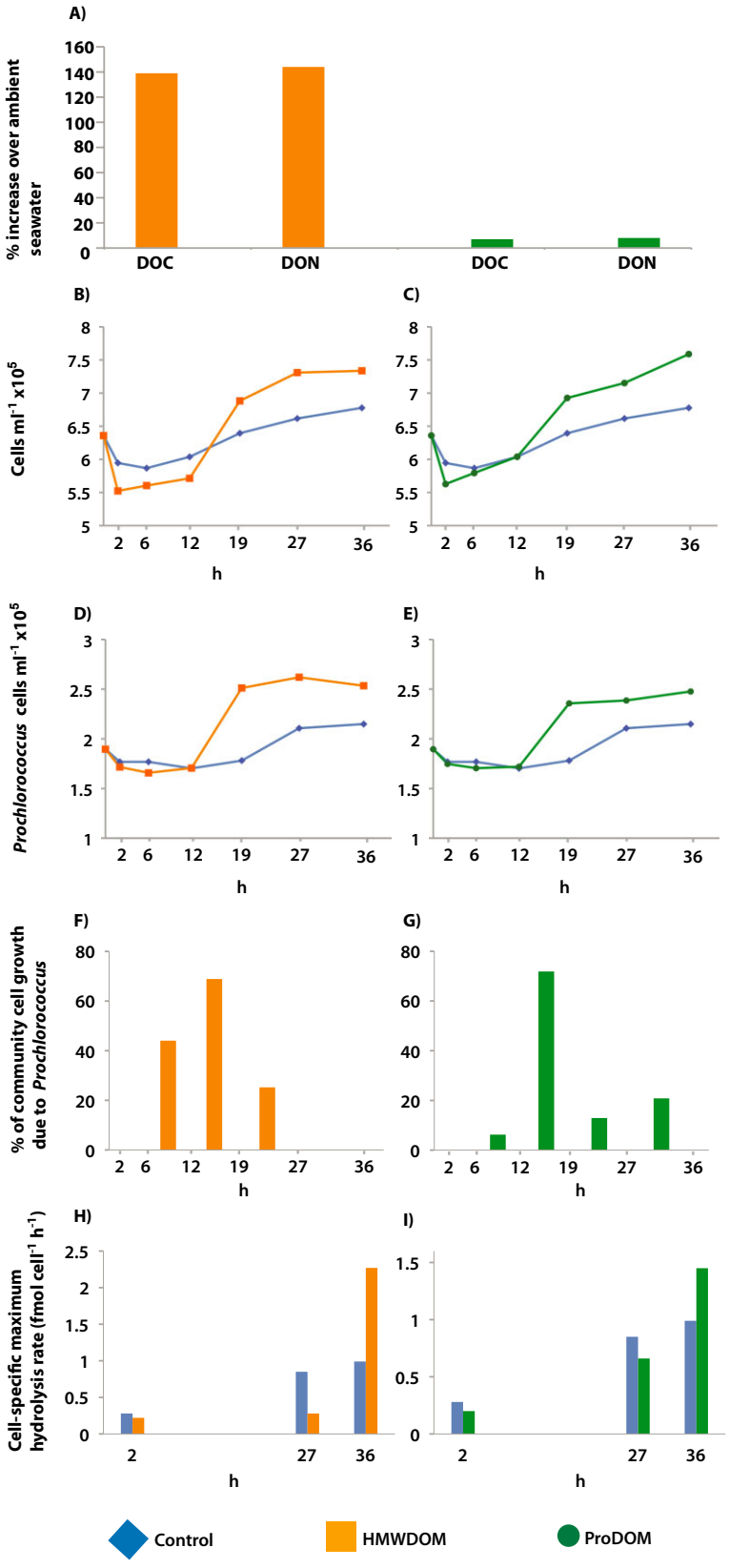

Fig. 1. Microbial community dynamics determined by flow cytometry and β-glucosidase exoenzyme assays. (A) Shows the percent increase over ambient seawater concentration of DOC and DON in microcosm perturbation experiments. For absolute concentrations and their standard deviations, see main text. Panels (B) HMWDOM and (C) ProDOM show total community cell counts, while panels (D) HMWDOM and (E) ProDOM show *Prochlorococcus*-like cell counts. Panels (F) HMWDOM and (G) ProDOM show *Prochlorococcus*-like cell growth as a percentage of total community growth that occurred within each of these treatments between consecutive time points. Panels (H) and (I) plot the cell-specific β-glucosidase activity for control and treatment microcosm communities through time.

Table 1. Read numbers and statistics.

Sample	Total reads[a]	Non-rRNA reads[b]	% rRNA[c]	NCBI hits[d]
cDNA				
0 h	618 918	369 456	38.2	249 185
Control 2 h	711 088	411 428	38.6	298 271
Control 12 h	616 224	431 332	28.4	294 160
Control 27 h	593 531	406 165	30.2	261 611
Control 36 h	602 581	417 565	29.3	255 126
HMWDOM 2 h	556 200	308 146	42.4	194 588
HMWDOM 12 h	564 333	401 107	27.6	278 836
HMWDOM 27 h	534 137	456 035	14.0	314 063
HMWDOM 36 h	573 227	462 651	18.4	297 466
ProDOM 2 h	654 338	472 796	26.3	357 097
ProDOM 12 h	647 187	255 872	57.8	176 581
ProDOM 27 h	638 776	432 165	30.5	323 866
ProDOM 36 h	585 229	439 791	23.1	289 130
DNA				
0 h	594 218	591 180	0.49	389 357
Control 36	638 559	635 073	0.50	430 104
HMWDOM 36	696 659	692 255	0.51	467 678
ProDOM 36	618 145	614 493	0.52	452 396

a. Total number of sequence reads per run.
b. Number of sequence reads after removal of rRNA sequences.
c. The percentage of the total number of sequenced reads that had a significant BLASTN match to rRNA.
d. Nonreplicate, non-rRNA reads with a significant BLASTX hit to proteins in the NCBI nonredundant database.

suggesting that the ProDOM treatment contained a higher proportion of labile DOM that could be converted into cellular biomass. Whereas the HMWDOM addition concentrated a fraction of the DOM already present in the sample, the ProDOM addition may have introduced exogenous DOM components to the community. Chemical analysis of the ProDOM material using high-performance liquid chromatography-electrospray ionization mass spectrometry (HPLC-ESI-MS) revealed the presence of 1491 low-molecular weight features with signal intensity at least fivefold greater than the maximum noise level. These features ranged in size from 100.2 to 1111.5 m/z, with the majority falling between 150 and 450 m/z. A control sample of Pro99 medium incubated without inoculation and processed as described in the experimental procedures for the ProDOM amendment, confirmed that these features were absent from the background medium.

Flow cytometric analysis indicated two stages of diauxic-like growth in the microbial community over the 36 h time course in both treatments relative to the control. The first and larger increase in cell numbers occurred between 12 and 19 h in both treatments relative to the control, where *Prochlorococcus* cells accounted for the majority of the total cell growth observed in treatments between these time points (Fig. 1B–G). The second, less pronounced growth stage in both DOM amended microcosms occurred between 19 and 36 h. Here, *Prochlorococcus* comprised a much smaller fraction of the total cell growth in the HMWDOM and ProDOM microcosms, indicating that heterotrophic bacterioplankton could be responsible for the later increases in cell numbers.

The final time point in both treatments was characterized by an increase in β-glucosidase exoenzyme activity (Fig. 1H and I) consistent with heterotrophic growth at later time points. β-glucosidase is an enzyme produced by heterotrophic picoplankton that catalyses the selective cleavage of glycosidic bonds in order to break down oligosaccharides into smaller sugars that can be transported into the cell. At the 36 h time point, assays indicated a 130% increase in activity in the HMWDOM treatment and a 46% increase in activity in the ProDOM treatment relative to the control. These findings indicate the presence of polysaccharides in both treatments, and the level of β-glucosidase activity per unit carbon added in each treatment suggests that labile polysaccharides likely comprised a substantial proportion of the DOC in the ProDOM amendment. The observed increase in β-glucosidase activity at the final time point in both treatments was likely related to heterotrophic growth and activity in the latter stages of the experiment.

Metagenomic and metatranscriptomic profiling of microcosm community structure

Table 1 outlines read numbers and database statistics for community DNA and cDNA samples sequenced from each of the different microcosms. Sequences derived from rRNA reads were identified *in-silico* and removed from all libraries, and taxonomic and functional annotations for the resulting non-rRNA reads were obtained from the top BLASTX hit against the National Center for Biotechnology Information-nonredundant (NCBI-nr)

database. The number of matches to a particular taxonomic group or NCBI-nr reference gene was normalized to the total number of reads with significant matches to the database, allowing for comparisons across samples.

Microbial community composition in the 35 m seawater used for our microcosm experiments (0 h DNA) was dominated by *Prochlorococcus* and *Pelagibacter* (Fig. 2A). Surface ecotypes of *Prochlorococcus* (Johnson *et al*., 2006) comprised approximately 50% of metagenomic reads with a significant BLASTx hit to the NCBI-nr database. The next most abundant group in our starting community was *Pelagibacter*, which accounted for 10% of assignable reads at 0 h. The vast majority of *Pelagibacter*-like sequences shared highest similarity to the *Pelagibacter ubique* HTCC7211 genome, a strain cultivated from the oligotrophic Sargasso Sea (Stingl *et al*., 2007). Metagenomic samples taken from 36 h indicated small increases in the relative abundance of a variety of heterotrophic groups in both HMWDOM and ProDOM relative to the control (Fig. 2B). These groups were the OM60 gammaproteobacteria, *Alteromonadales*, *Rhodobacterales*, SAR116 and *Flavobacteriales*. DNA sequences from the SAR11 group increased in the ProDOM treatment by nearly 50% over the control, suggesting a preference for this DOM source.

Prochlorococcus and *Pelagibacter* appeared to be the most transcriptionally active taxa in our experiment, as indicated by the proportion of assignable reads belonging to these two groups in the 0 h cDNA library (Fig. 2A). cDNA libraries from subsequent time points indicated subtle changes in taxonomic activity over time in DOM-enriched microcosms relative to the control. While these temporal sequence data indicated only minor changes in taxonomic profiles in response to DOM perturbations on this short timescale, changes in gene expression patterns within the ambient microbial community at Station ALOHA were more pronounced. Figure 2C shows the taxonomic association of differentially expressed NCBI-nr genes that were significantly enriched (posterior probability of ≥ 0.9) in cDNA samples from the treatments relative to the control at each time point, where significantly underrepresented genes were excluded. From a taxonomic perspective, both treatments exhibited a similar temporal trend in differential gene expression. Across the first three time points, the majority of differentially expressed transcripts were associated with *Prochlorococcus*. *Pelagibacter* demonstrated rapid responses in both treatments, with more consistent activity captured in the HMWDOM treatment, where there was an increase in differentially expressed transcripts at 27 h. The later time points indicated increasing transcript abundances from different heterotrophic taxa, particularly *Alteromonadales* and the OM60 clade, and these signals were typically observed earlier in ProDOM relative to HMWDOM. These taxonomic trends in differential gene expression mirrored the microbial community growth and abundance patterns (Fig. 1B–G), where *Prochlorococcus*-like cells represented the majority of growth at earlier time points, but not later. Combined with high β-glucosidase activity at 36 h (Fig. 1H and I), these independent methods of analysis support the hypothesis that a microbial succession in growth and activity occurred in our treatments in response to DOM perturbations. Abundant, oligotrophic taxa (*Prochlorococcus* and *Pelagibacter*) were observed to rapidly respond to changes in the ambient DOM pool. In contrast, the opportunistic heterotrophic taxa (OM60, *Alteromonadales*, etc.) appeared to gradually increase in abundance, and their transcriptional responses became more apparent in the latter stages of the incubation.

Taxon-specific responses to DOM perturbations inferred from genome-centric transcriptomic analyses

To gain additional insight into microbial community dynamics and the DOM substrate utilization patterns driving the microbial successions previously described, we performed differential gene expression analyses on changes in relative transcript abundance within specific taxonomic bins. We focused on those taxa with the greatest percentages of differentially expressed genes (relative to the control; Fig. 2C), which were *Prochlorococcus*, *Pelagibacter* and gammaproteobacteria from the OM60 clade.

Prochlorococcus

DOM enrichments induced specific, rapid changes in *Prochlorococcus* gene expression in biosynthetic pathways as supported by the significant differential expression (DE) of KEGG orthologs (KOs) that were enriched in treatments (Fig. 3A). Both DOM additions appeared to trigger a burst in protein biosynthesis in *Prochlorococcus* as the vast majority of DE KOs in the pathways ribosome and translation factors occurred at the 2 h time point in both treatments (Datasets S2 and S3). *Prochlorococcus* also exhibited an immediate and sustained increase in the DE of KOs from pathways involved in genome replication and cell division (Fig. 3A). The expression of KOs from lipid and starch biosynthesis pathways was also significantly more abundant in DOM-enriched microcosms, suggesting increased levels of membrane biogenesis and carbon storage (Fig. 3A). The greater number of DE KO's for protein, cell division and lipid biosynthesis pathways in ProDOM, combined with their higher percent increase relative to the HMWDOM treatment, indicates that the magnitude of response by *Prochlorococcus* at the level of gene expression was more pronounced for ProDOM (Fig. 3A). These observations support the hypothesis

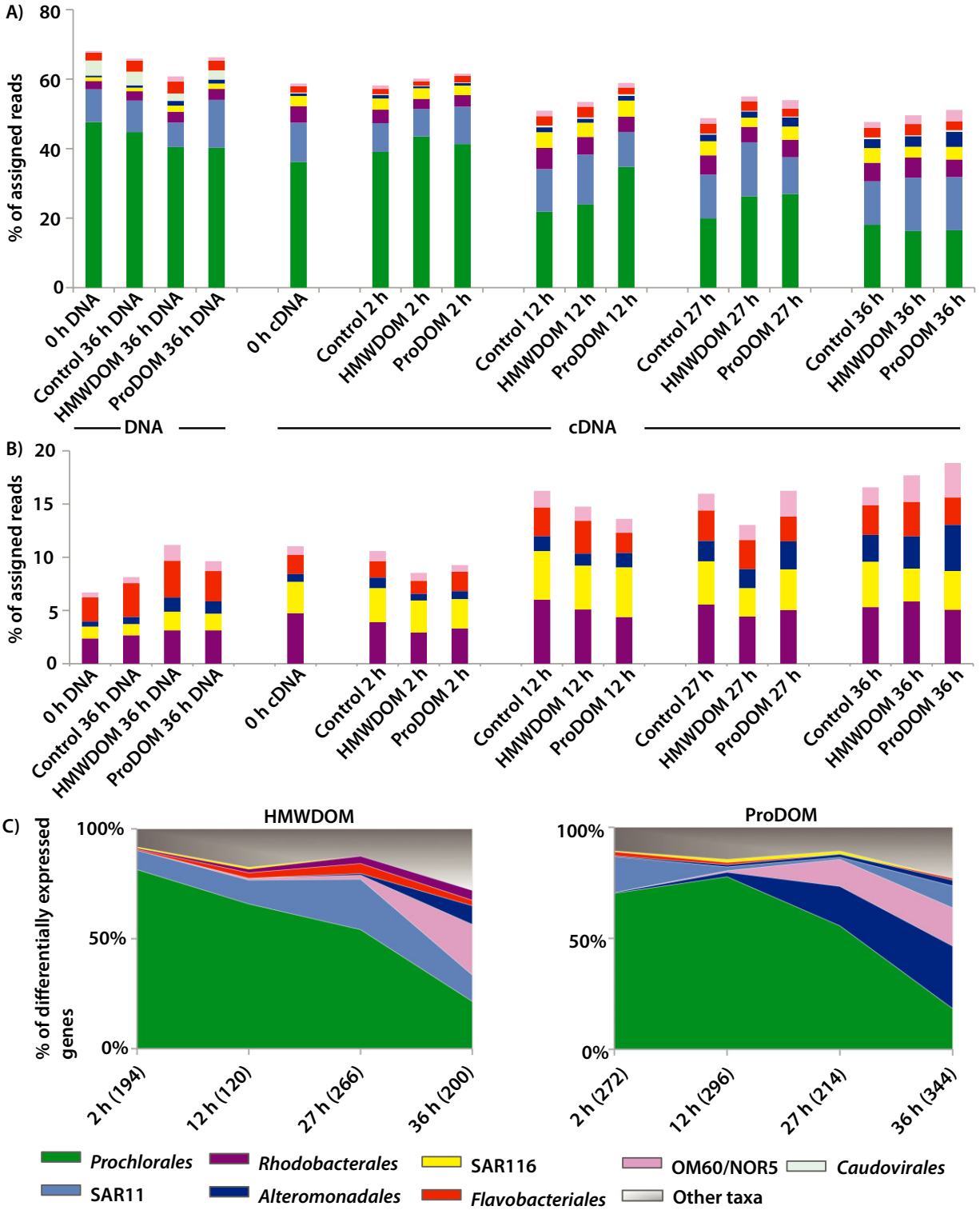

Fig. 2. NCBI order level taxonomy of DNA and cDNA reads through time. (A) Proportion of the total number of assignable reads represented by a taxonomic order in DNA and cDNA libraries. Only those groups that represented > 3% of assignable reads are shown. (B) The same as in (A) but only for selected heterotrophic taxa. (C) The taxonomic association of those NCBI-nr genes detected as significantly enriched in cDNA from treatments relative to controls at each time point show which taxa exhibited changes in gene expression in response to DOM addition. The numbers in brackets along the *x*-axis denote the total number of NCBI-nr genes detected as significantly enriched in the treatment at each time point. All taxa shown in (A) are present in (C) with the exception of *Caudovirales*. Taxonomic representation of reads at the order level was chosen to visually reduce the number of taxa represented on the plots, while simultaneously represent genomes from key divisions.

A) *Prochlorococcus*

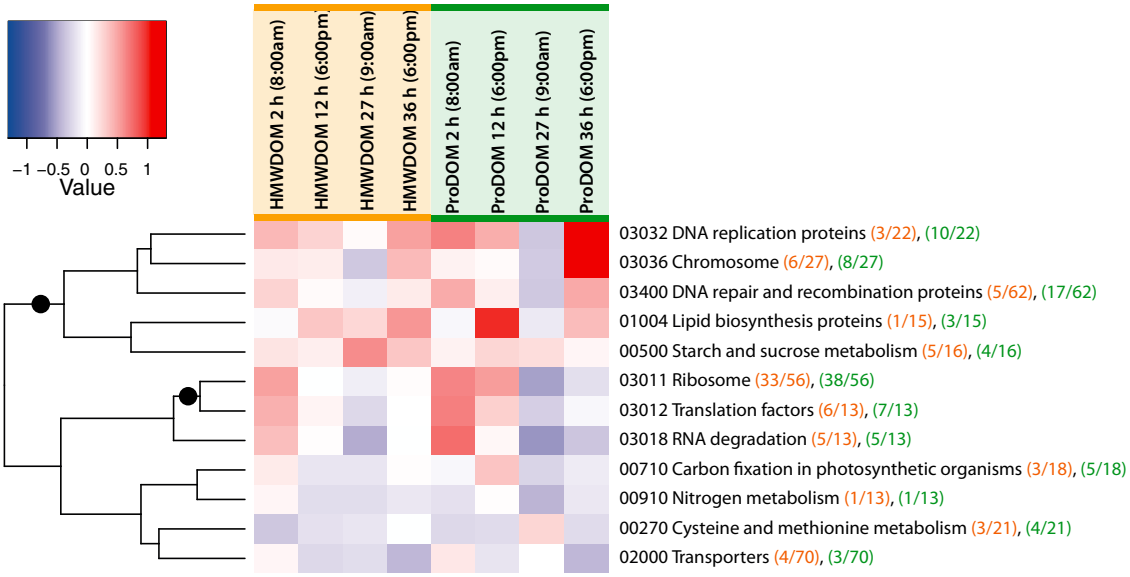

B) *Pelagibacter*

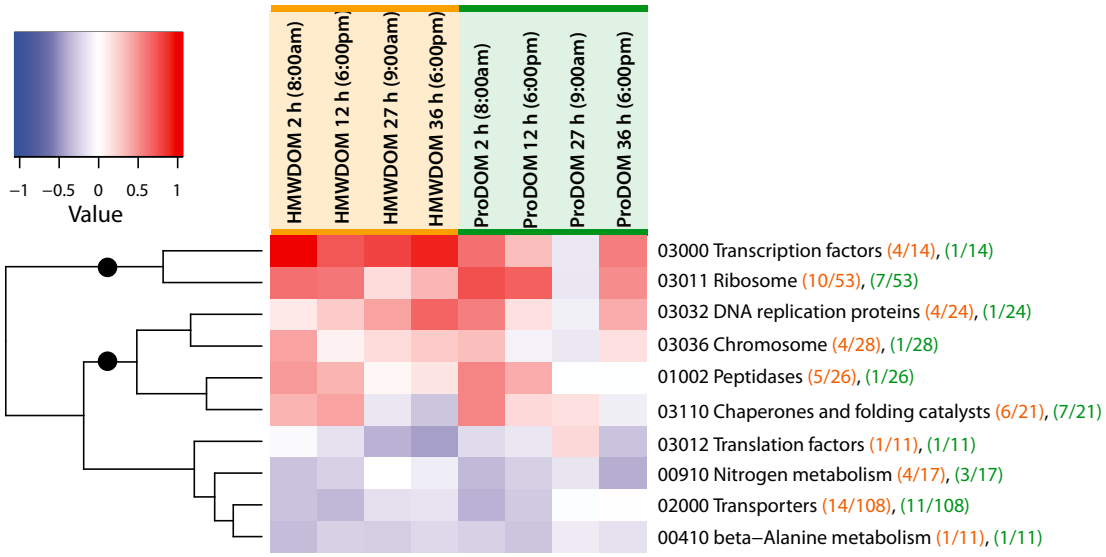

Fig. 3. Heatmaps depicting the relative abundance of metabolic pathways in the metatranscriptome of various taxonomic groups over time for both DOM treatments. Pathway abundances for cDNA reads from each sample were calculated as a fraction of sequences mapping to a pathway over the total number of cDNA hits for a particular taxon with a significant match in KEGG. Level 3 pathway abundance is calculated as the percent change in the treatment relative to the control (% treatment – % control/% control), such that a value of 1 in the heatmap represents a 100% increase in a pathway in the treatment relative to the control. The dendrogram clusters pathways by similar mean abundance values. Note that all time points occurred during daylight hours.
A. *Prochlorococcus* transcriptome. Only those pathways that have significant differentially expressed KOs that were either enriched or underrepresented in both treatments relative to the control in at least three of the four time points are shown.
B. *Pelagibacter* transcriptome. The criteria for choosing pathways to display for *Pelagibacter* was slightly different from *Prochlorococcus*, in that only one treatment had to have DE KOs at three of four time points, rather than both. This was due to the decreased sequencing depth in *Pelagibacter*. Conflicting pathways that contained differentially expressed KOs that were both enriched and underrepresented in treatments at three of four time points are excluded. The clusters indicated by the black dots represent pathways enriched in the treatment by these criteria, and the remainder are those that were underrepresented. The numbers in brackets next to the pathway names (x/y) indicate the total sum of KOs detected as differentially expressed (x) over the total number of KOs detected in that pathway (y) across all time points for HMWDOM (orange) and ProDOM (green). Note that DE KOs are sometimes assigned to multiple pathways encoding similar metabolic functions (e.g. DNA replication proteins and chromosome). Therefore, combining the number of DE KOs from two pathways does not always equal the sum of the numbers in brackets.

Table 2. Number of *Prochlorococcus* and *Pelagibacter* ortholog clusters detected as differentially expressed (DE) in cDNA samples[a].

Organism and Treatment	Total DE +[b]	Core DE +[c]	Auxiliary DE +[d]	Unassigned DE +[e]	Total DE –	Core DE –	Auxiliary DE –	Unassigned DE –
Prochlorococcus								
HMWDOM	301/2743	114 (38%)	23 (8%)	164 (54%)	130/2743	72 (55%)	11 (9%)	47 (36%)
ProDOM	444/2743	174 (39%)	35 (8%)	235 (53%)	211/2743	113 (54%)	22 (10%)	76 (36%)
Pelagibacter								
HMWDOM	100/1950	50 (50%)	17 (17%)	33 (33%)	46/1950	25 (55%)	2 (4%)	19 (41%)
ProDOM	63/1950	32 (51%)	9 (14%)	22 (35%)	44/1950	23 (52%)	3 (7%)	18 (41%)

a. The total number of ortholog clusters detected in all cDNA samples was 2734 for *Prochlorococcus* and 1950 for *Pelagibacter*. Those orthologs that were significantly enriched in treatments relative to controls are indicated by + and those that were significantly underrepresented as – . The number of ortholog clusters detected as DE in *Pelagibacter* is lower due to decreased sequencing depth compared to *Prochlorococcus*.
b. Total DE refers to the total number of orthologs detected as DE as either enriched (+) in treatments relative to controls, or underrepresented (–).
c. Core DE refers to the total number of orthologs detected as DE in a core pathway involved in central metabolic processes and the number in brackets represents their fraction of total DE orthologs.
d. Auxiliary DE refers to the total number of orthologs detected as DE in an auxiliary pathway and the number in brackets represents their fraction of total DE orthologs.
e. Unassigned DE refers to the total number of DE orthologs that were not assigned to KEGG level 3 pathways and the number in brackets represents their fraction of total DE orthologs.

(also supported by the flow cytometry data) that ProDOM contained a greater amount of labile DOM, despite the higher quantity of carbon supplied in the HMWDOM treatment (Fig. 1A).

The *Prochlorococcus* population in the control microcosm appeared to dedicate a greater fraction of its transcriptome to nitrogen acquisition and assimilation relative to the treatments. KOs involved in nitrogen metabolism and transport pathways were significantly underrepresented in treatment samples (Fig. 3A), including but not limited to the ammonium assimilation protein glutamine synthetase, and both the permease and substrate-binding subunits of the Urea ABC transporter. Additionally, transcripts encoding an ammonium transporter ortholog unassigned in KEGG represented the only *Prochlorococcus* ortholog that was significantly underrepresented in both treatments at every time point (see Cluster 287, Datasets S2 and S3). These nitrogen acquisition genes are highly expressed by *Prochlorococcus* as a nitrogen scavenging response to nitrogen stress in culture (Tolonen *et al*., 2006), and their underrepresentation in treatments could indicate that both DOM treatments provided a labile source of DON.

To obtain a better understanding of the DOM utilization patterns that contributed to the physiological responses observed in *Prochlorococcus*, the DE of orthologs belonging to auxiliary KEGG pathways (as opposed to core pathways involved in central metabolic processes) was examined in greater detail. The number of DE *Prochlorococcus* orthologs binned into these two pathway categories (auxiliary vs. core) is presented in Table 2, and details regarding KEGG pathway assignments as core or auxiliary are presented in Supporting Information Files S1 and S2. At 2 h, *Prochlorococcus* transcripts mapping to the KO D-amino acid oxidase exhibited an ~ 8-fold increase in both treatments relative to the control (Tables S1 and S2). This KO catalyses the breakdown of D-amino acids into their corresponding oxoacids and ammonium, and its increased activity suggests a source of proteinaceous material common to both treatments, perhaps in the form of peptidoglycan. Breakdown of D-amino acids should directly correspond to an increase in glutamine and glutamate via GS-GOGAT ammonium assimilation (Muro-Pastor *et al*., 2005). An increase in cellular concentrations of glutamate is supported by the DE of a number of KOs involved in the biosynthesis of aspartate, proline and arginine – amino acids that use glutamate as a metabolic precursor (Tables S1 and S2). The enrichment of various DE orthologs encoding peptidases and proteases was also observed in treatment transcriptomes, suggesting *Prochlorococcus* was capable of the uptake and degradation of oligopeptides present in the DOM additions. Transcripts for five different *Prochlorococcus* proteases were exclusively enriched in the ProDOM treatment, and four of them were enriched at 2 h, indicating a rapid response to an influx of protein. These observations once again indicate that the *Prochlorococcus*-derived DOM fraction we employed was richer in labile protein material than HMWDOM derived from surface seawater, despite the large discrepancy in organic carbon quantity (Fig. 1A).

Pelagibacter

Similar to *Prochlorococcus*, *Pelagibacter* also exhibited rapid changes in gene expression in response to both HMWDOM and ProDOM enrichment. The majority of DE KOs involved in protein biosynthesis pathways occurred at the 2 and 12 h time points in both treatments (Fig. 3B, Datasets S4 and S5). The *Pelagibacter* population also

demonstrated transcriptional growth signals in response to DOM perturbation (Fig. 3B) with DE KOs falling into the categories of DNA replication proteins and chromosome.

Also like *Prochlorococcus*, *Pelagibacter* cells responded to DOM addition by decreasing the expression of orthologs involved in nitrogen acquisition. These included DE KOs from the pathway nitrogen metabolism (Fig. 3B, Datasets S4 and S5), such as the ammonium assimilation protein glutamine synthetase and two paralogs of the glycine cleavage system T protein that could be involved in nitrogen acquisition via the breakdown of methylated organic nitrogen substrates (Sun *et al*., 2011). Transporters were significantly underrepresented in *Pelagibacter* in both DOM treatments (Fig. 3B). The majority of these DE KOs and other DE transport orthologs unannotated in KEGG were annotated in NCBI-nr as functioning in the uptake of organic or inorganic nitrogen-containing compounds (Tables S3–S6).

Similar to *Prochlorococcus*, the underrepresentation of *Pelagibacter* transcripts related to nitrogen acquisition may also indicate that DOM additions provided a source of organic nitrogen. To gain further insight into *Pelagibacter* DOM substrate utilization, we examined differentially expressed KOs belonging to auxiliary pathways outside of those core pathways involved in central metabolic processes (see Table 2 for ortholog counts and Supporting Information File S2 for pathway designations). The gene encoding formate-tetrahydrofolate ligase (*fhs*) was significantly enriched in *Pelagibacter* transcripts from the HMWDOM treatment at the 27 h time point (Table S7) and was on average 62% higher than the control across all time points, suggesting an influx of C1 groups entering the tetrahydrofolate (THF) oxidation pathway. Whereas transporters were generally underrepresented in the treatments, a few transporters appeared to be stimulated by the DOM additions (Tables S5 and S6). In the HMWDOM treatment, we observed significant enrichment of transcripts for the gene encoding the PheC transporter (Table S5), which is linked to the sarcosine oxidase operon in multiple *Pelagibacter* genomes. The DE of *fhs* and *pheC* potentially link the uptake of methylated organic nitrogen compounds, like sarcosine, to C1 oxidation in *Pelagibacter*, providing a mechanism for nitrogen acquisition and the production of energy needed to fuel the growth signals observed in KEGG pathways (Fig. 3B).

In the ProDOM treatment, two *Pelagibacter* orthologs involved in homocysteine biosynthesis were enriched at the 2 h time point (Table S8). These were homoserine O-acetyltransferase (*metX*) and O-acetylhomoserine (thiol)-lyase (*metY*). Homocysteine is required by the enzyme betaine-homocysteine methyltransferase (BHMT) for the first demethylation step in glycine betaine degradation (Barra *et al*., 2006). The gene encoding BHMT was not detected as differentially expressed over the entire course of the experiment (likely due to its low representation among SAR11 transcripts); however, its expression was fourfold higher in ProDOM relative to the control at 2 h (posterior probability = 0.63). Transcripts for a gene annotated as γ-butyrobetaine dioxygenase (*γ-bbh*) was enriched in ProDOM at 12 h, and this protein catalyses the first step in the degradation of γ-butyrobetaine, a substance whose degradation results in the production of glycine betaine (Kleber, 1997). In the *Pelagibacter* HTCC7211 genome, homologs encoding subunits of an L-proline/glycine betaine ABC transporter are linked to the *γ-bbh* gene. Together these observations suggest that the ProDOM treatment provided a source of γ-butyrobetaine- and glycine betaine-like substrates, thereby supplying *Pelagibacter* with a source of both nitrogen and energy.

OM60 clade

Of the 3666 OM60 clade ortholog clusters identified among the sequenced data (Dataset S1), 37 were detected as differentially expressed in cDNA samples from the HMWDOM treatment and 70 were detected from the ProDOM treatment. The vast majority of these DE orthologs occurred at the 27 and 36 h time points, and those enriched in treatments included orthologs from KEGG pathways involved in protein, nucleotide and peptidoglycan biosynthesis (Tables S9 and S10). These later time points also coincided with the growth of non-*Prochlorococcus*-like cell types in treatments as determined by flow cytometry data and increasing activity of β-glucosidase (Fig. 1).

Interestingly, differentially expressed orthologs indicate OM60 polysaccharide utilization in both DOM treatments. Transcripts for a predicted beta-glucoside-specific TonB-receptor (cluster 4450) was enriched in both treatments at 27 and 36 h (Tables S9 and S10). In the HTCC2148 genome, this TonB receptor homolog is located downstream of a glycosyl hydrolase (GH) gene, which was significantly enriched in OM60 transcripts in the HMWDOM treatments at 27 h. Further examination of this GH homolog from the HTCC2148 genome using the database for carbohydrate-active enzyme annotation (http://csbl.bmb.uga.edu/dbCAN/) found the signature catalytic motif EXDXXE of the GH16 family (http://www.cazypedia.org/index.php/Glycoside_Hydrolase_Family_16, Michel *et al*., 2001), which is also present in the transcripts mapping to this region of the gene in both treatments. Enzymes of the GH16 family are known to cleave β-1,3 linked glucans and galactans (Baumann *et al*., 2007; Hehemann *et al*., 2010), which are often abundant in HMWDOM (Aluwihare *et al*., 1997). GH16 enzymes preferentially hydrolyse longer-chain substrates, which could have provided the shorter oligosaccharides that induced β-glucosidase enzyme activity in the treatments (Fig. 1H and I).

In accordance with signals for polysaccharide utilization and uptake, OM60 transcripts from the ProDOM treatment (Table S10) showed enrichment in genes encoding glycolysis (enolase and pyruvate kinase at 27 h) and citric acid cycle enzymes (isocitrate dehydrogenase and succinyl-coenzyme A synthetase at 36 h). That similar signals were not observed in HMWDOM (Table S9) may indicate a slower response time in this treatment compared with ProDOM. This hypothesis is supported by the higher proportion of OM60 transcripts relative to the entire community in ProDOM cDNA samples at 27 and 36 h (Fig. 2A) and the greater number of DE orthologs in this treatment. These observations once again suggest that the ProDOM amendment contained a higher concentration of more labile substrates, which may have accelerated the rate at which the heterotrophic population was able to respond.

Discussion

We investigated the response of an oligotrophic microbial community to two organic carbon sources using controlled microcosm experiments in the NPSG. Both treatments induced similar patterns in cell growth, taxonomic response and exoenzyme activity despite differences in the quantity and quality of the carbon added. These observations suggest that ProDOM contained a greater proportion of labile carbon relative to HMWDOM, which represented a standing stock of semilabile and refractory organic carbon subjected to persistent heterotrophic activity. This hypothesis is supported by transcriptional signals that indicate a stronger response to ProDOM by *Prochlorococcus* and the OM60 clade.

Relative to the control, the *Prochlorococcus* transcriptional responses from treatment microcosms indicated that DOM enrichments provided DON substrates in the form of proteinaceous material, which appeared linked to an increase in gene expression in biosynthetic pathways and a decrease in the expression of genes involved in nitrogen acquisition. Studies have shown that *Prochlorococcus* utilizes various nutrient acquisition strategies to circumvent nitrogen and phosphorus depletion (Martiny *et al*., 2006; 2009), and highlighted the ability of this cyanobacterium to utilize organic nutrients for growth (Martínez *et al*., 2012; del Carmen Muñoz-Marín *et al*., 2013; Gómez-Pereira *et al*., 2013). Some studies suggest that the ecological success of *Prochlorococcus* in oligotrophic regions of the ocean is due in part to their high uptake rate of amino acids (Zubkov *et al*., 2004; Mary *et al*., 2008), which can account for 33% of the total bacterioplankton turnover of these compounds in oligotrophic parts of the Arabian Sea (Zubkov *et al*., 2003). These authors note that the classical distinction between autotrophic and heterotrophic organisms in the marine environment is blurred in oligotrophic waters where photosynthetic cyanobacteria often demonstrate mixotrophic tendencies by utilizing organic nutrients.

Similar to the *Prochlorococcus* population, *Pelagibacter* transcriptional responses in the treatments also indicated the utilization of DON substrates. *Pelagibacter* transcriptional signals for the utilization of methylated organic nitrogen compounds in the treatments appeared linked to the enrichment of transcripts from genes involved in biosynthetic processes and the underrepresentation of genes involved in nitrogen acquisition. *Pelagibacter* is capable of the uptake and degradation of a wide variety of one-carbon compounds including methyl functional groups from methylated compounds, which provide a source of energy via the C1 THF oxidation pathway (Sun *et al*., 2011). Our results suggested that in addition to an energy source, *Pelagibacter* could utilize methylated organic nitrogen compounds from the ambient DOM pool to acquire nitrogen. A metaproteomic study conducted in the euphotic zone of the seasonally phosphorus-limited Sargasso Sea found that the periplasmic substrate-binding protein for phosphonate acquisition was among the most frequently detected *Pelagibacter* proteins (Sowell *et al*., 2009), indicating that these organisms rely on the ambient DOM pool for survival under nutrient poor conditions.

OM60 clade transcripts in the treatment microcosms were significantly enriched relative to the control at later time points, and involved genes in polysaccharide degradation and various biosynthetic processes. Whereas abundant taxa like *Prochlorococcus* and *Pelagibacter* demonstrated rapid responses to DOM enrichment, the OM60 population represented a low abundance group that responded at later time points. Many studies have shown that opportunistic, low abundance taxa bloom under increasing concentrations of organic nutrients (Cottrell and Kirchman, 2000; Eilers *et al*., 2000; McCarren *et al*., 2010; Romera-Castillo *et al*., 2011; Tada *et al*., 2011; Nelson and Carlson, 2012). These opportunistic taxa exhibit a 'feast or famine' lifestyle (Nissen, 1987; Flärdh *et al*., 1992; Srinivasan and Kjelleberg, 1998), and are often referred to as copiotrophs (Lauro *et al*., 2009; Yooseph *et al*., 2010). We suggest that oligotrophic conditions at Station ALOHA were likely responsible for the low abundance and activity of copiotrophs like members of the OM60 clade, and that exposure to elevated concentrations of organic nutrients allowed this population to gradually increase in numbers, such that their transcriptional responses became more apparent in the latter stages of the incubation.

McCarren and colleagues (2010) conducted a similar HMWDOM microcosm experiment within the mixed layer of the NPSG; however, results from that study showed rapid and strong responses in copiotrophic taxa, particu-

larly among organisms of the *Alteromonadales*. Differences in response dynamics between that study and the one presented here are likely the result of multiple variables. The McCarren and colleagues treatment had a DOC concentration that was 300% greater than ambient conditions, more than double the amount of HMWDOM used here, and the percent abundance of cDNA reads from *Alteromonadales* was 300% greater in the starting community of that experiment relative to that observed in our experiments. These two variables implicate a potential founder effect for an organism known to have rapid growth kinetics under increasing substrate concentrations (Eilers *et al*., 2000).

A major challenge in microbial oceanography is to understand the mechanisms driving changes in community composition and activity across temporal and seasonal time scales (Fuhrman *et al*., 2006; Giovannoni and Vergin, 2012; Ottesen *et al*., 2013). In areas where seasonal stratification of the water column regularly occurs (Karl *et al*., 2012), an extremely oligotrophic microbial assemblage can result because of inorganic nutrient depletion. Amendment of such an assemblage with two distinct DOM sources indicated that numerically dominant oligotrophic microbes have the ability to rapidly acquire nitrogen from organic sources and implicates the importance of carbohydrates within the DOM pool for sustaining less abundant copiotrophic microorganisms in these systems.

Experimental procedures

Experimental set-up and sample collection

Seawater for microcosm incubation experiments was collected at 22°45′N, 158°00′W from the bottom of the mixed layer (35 m) at dawn, on 27 May 2010. Hydrocasts for sampling were conducted using a conductivity-temperature-depth (CTD) rosette sampler aboard the R/V *Ka'imikai-o-Kanaloa*. Water was transferred to pre-acid-washed, sample-water rinsed 20 l polycarbonate bottles. The deck-board incubator was a blue light type, which simulated light levels at ca. 10 m (roughly 35% surface irradiance). Twenty litre carboys were wrapped in a single layer of black fibre glass screen, to further decrease the light level inside the carboys to 14% surface irradiance, the *in situ* light intensity at 25–45 m. Carboys were incubated in deck-board incubators supplied with flow-through surface seawater to maintain near *in situ* temperatures. The control microcosm consisted of 20 l of 35 m water, and for the treatments, 2 l of DOM concentrate (HMWDOM or ProDOM) was added to 18 l of water obtained from 35 m depth for a total volume of 20 l.

RNA and DNA sampling

At selected time points, bacterioplankton biomass from ~ 2 l of sample water was rapidly collected for RNA extraction by first pre-filtering through a 1.6 μm glass fibre filter and then harvesting cells onto 0.2 μm Sterivex (Millipore, Billerica, MA, USA) filters. Filtration was limited to 10 min or less. 1.8 ml of RNAlater® (Applied Biosystems, Life Technologies: Grand Island, NY, USA) was added to the filter, which was subsequently capped and flash frozen at −80°C. Samples were transported frozen in a dry shipper and stored at −80°C until RNA extraction procedures. At both the beginning and end of the experiment, biomass was similarly collected for DNA samples. Eighteen litres of seawater for T0 DNA sample collection were directly taken from the CTD bottle (not from the microcosms), and 5–6 l of water were filtered from the end of the experiment for DNA extractions. Filter units for DNA extraction were filled with lysis buffer (50 mM Tris-HCl, 40 mM ethylenediaminetetraacetic acid and 0.75 M sucrose), capped and frozen at −20°C until extraction.

RNA extraction

Total RNA was extracted using the *mir*Vana miRNA Isolation kit (Ambion, Life Technologies) with modification to account for the recovery of RNA from Sterivex filters. Filters were thawed on ice, and at which point RNAlater® was expelled via syringe and discarded. 1.5 ml of lysis/binding buffer was added to the filter, which was resealed and vigorously vortexed for 1 min. One hundred fifty microlitres of miRNA homogenate additive was added, and after vortexing, the filter was incubated on ice for 10 min. The resulting lysate was removed with a syringe and divided into two 2 ml tubes, which were processed separately through the remainder of the standard *mir*Vana miRNA isolation kit protocol. Following purification of the total RNA from the *mir*Vana columns, samples resulting from a single filter were combined back together for genomic DNA removal with TURBO DNA-free (Ambion, Life Technologies), then purified and concentrated using the RNeasy MinElute cleanup kit (Qiagen, Valencia, CA, USA).

DNA isolation

Total DNA was extracted and purified using the Quick-Gene 610 l system (Fujifilm, Tokyo, Japan) and DNA Tissue Kit L (Autogen, Holliston, MA, USA) with a modified lysis protocol. Fifty milligram of lysozyme was added to 1 ml of lysis buffer (described above), mixed by vortexing before 40 μl was added to thawed Sterivex filters. Filters were set in a rotating incubator at 37°C for 45 min. Following this, 100 μl each of the kit buffers EDT and MDT were added to the filter, which was incubated at 55°C for 2 h with rotation. The lysate was decanted from the filter using a syringe; 2 ml LDT solution was added to the lysate, mixed by inversion and incubated at 55°C for a further 15 min without rotation. 2.7 ml EtOH was added and vigorously mixed by vortexing, at which point the sample was immediately loaded onto the QuickGene column and placed in the Quick-Gene 610 l instrument (Fujifilm, Tokyo, Japan) for purification according to the manufacturer's DNA Tissue protocol, with an elution volume of 400 μl.

rRNA subtraction, RNA amplification, cDNA synthesis

Ribosomal RNA transcripts were removed from total RNA extracts using a subtractive hybridization protocol published

in Stewart and colleagues (2010) with slight modifications. Bacterial and archaeal 16S and 23S rRNA probes were separately amplified from DNA sampled from 0 h and 36 h microcosm communities using 50 μl Herculase II Fusion DNA polymerase reactions and 30 ng of template DNA. Polymerase chain reaction (PCR) products from these individual reactions for each subunit were pooled together for PCR purification via the QIAquick PCR purification kit (Qiagen), eluted with 30 μl and DNA was quantified using a ND-1000 spectrophotometer (Nanodrop technologies, Wilmington, DE, USA). Each elution was dried by speed vac (Savant; Thermo Scientific: Asheville, NC, USA) and concentrated to obtain the 250–500 ng required for the *in vitro* transcription to generate biotin labelled antisense rRNA probes. Hybridization reactions containing 150 ng of total community RNA was hybridized with 1200 ng of rRNA probe master mix, which was comprised of 450 ng each bacterial and 150 ng each archaeal small- and large-subunit rRNA probes. Probe removal was performed as indicated in Stewart and colleagues (2010).

Purified and concentrated rRNA subtracted RNA was linearly amplified and converted to cDNA using the MessageAmp II-Bacteria kit (Ambion) following the manufacturer's instructions and as originally described in Frias-Lopez and colleagues (2008). Samples containing 9–25 ng of RNA were polyadenylated using *Escherichia coli* poly(A) polymerase I. Poly(A)-tailed RNA was reverse transcribed using the oligo(dT) primer T7-BpmI-d$(T)_{16}$VN (5′-GCCAGTGAATTGTAATACGACTCACTATAGGGGCGAC TGGAGTTTTTTTTTTTTTTTTVN-3′), which contains a promoter sequence for T7 RNA polymerase and a recognition site for the restriction enzyme *Bpm*I. cDNA templates were transcribed *in vitro* (37°C for 6 h) resulting in microgram quantities of antisense RNA (aRNA). The aRNA was then converted to double-stranded cDNA. First strand synthesis was performed using the SuperScript III First-Strand Synthesis System (Invitrogen, Carlsbad CA, USA) using random hexamer priming, and second strand synthesis was accomplished using the SuperScript Double-Stranded cDNA synthesis kit (Invitrogen). cDNA was purified with the QIAquick PCR purification kit (Qiagen) before digestion with *Bpm*I for 3 h at 37°C to remove poly(A)-tails, after which *Bpm*I was heat inactivated at 70°C for 20 min.

Pyrosequencing

Pyrosequencing was performed using Titanium series chemistry on a Roche Genome Sequencer FLX instrument (Indianapolis, IN, USA). Library construction followed the Titanium Rapid Library Preparation protocol. To obtain a size distribution of cDNA molecules that also contained smaller fragments, adaptor-ligated libraries were not diluted before size selection with AMPure XP beads. Library concentrations were determined using the Titanium slingshot kit (Fluidigm, San Francisco, CA, USA) and added to emulsion PCR reactions at 0.1 molecules per bead. 454 Life Sciences (Roche) standard protocols were used for sequencing and quality controls. The sequences reported in this paper have been deposited in the NCBI sequence read archive under study SRP021115.

Flow cytometry

At each time point, 5 μl of 25% grade 1 glutaraldehyde (Sigma, Saint Louis, MI, USA) was added to 1 ml of seawater, mixed by inversion, incubated at room temperature for 10 min, then flash frozen in liquid N_2 and stored at –80°C. Samples were thawed in the dark, and cell counts were performed using an Influx cytometry platform (Becton Dickinson, Franklin Lakes, NJ, USA). *Prochlorococcus*-like cells were identified based on their unique red autofluorescence and scatter signals, using a 692 nm laser and vertical forward scatter. Prior to total cell counts, samples were stained with SYBR Green (Invitrogen) for 10 min, and DNA-containing cells were identified based on SYBR fluorescence using a 530 nm laser and scatter signals (Marie *et al*., 1997). A minimum of 20 000 *Prochlorococcus*-like cells and 35 000 SYBR stained cells were counted per sample, where the count error based on a Poisson distribution is less than 1% of counts. Flow cytometry count data were analysed using FlowJo software (Tree Star, Ashland, OR, USA).

Exoenzyme assay

β-glucosidase activity was measured as an increase in fluorescence of the product 4-methylumbelliferone (MUF) released after enzymatic hydrolysis of the nonfluorescent 4-methylumbelliferyl-β-D-glucopyranoside (MUF-Glc; Sigma-Aldrich, Saint Louis, MI, USA) substrate. The kinetic parameters of β-glucosidase activity for each time point were measured in a series of eight different MUF-Glc concentrations, ranging from 0.05 to 100 μM (final concentration). The highest concentration (in this case, 100 μM) was saturating and was performed in triplicate for each sample individually. Summarized across all triplicate samples, the mean of the standard error was 1.4% and the SD of all the standard errors obtained was ±1.4% indicating low levels of variability.

The kinetic parameters were determined using the Hanes–Woolf plot graphical representation of the rearrangement of the Michaelis–Menten equation as follows: $S:V = K_m:V_m + S:V_m$, with the MUF-Glc concentration (S), the hydrolysis rate (V), the maximum hydrolysis rate (V_m) and the half-saturation constant (K_m). All samples were incubated in the dark at *in-situ* temperature in an incubator. Hydrolysis of MUF-Glc to MUF (excitation and emission: 359 and 449 nm respectively) was measured on a Perkin Elmer LS-5 spectrofluorometer (Waltham, MA, USA). At least four measurements were obtained within 18 h to verify the linearity of the assay. A standard curve using MUF (Sigma-Aldrich) from 0 to 500 nM in 0.2 μm filtered and boiled seawater was used to calculate hydrolysis rates. Blanks (i.e., ultrapure water) and killed controls (i.e., sample fixed with 0.2% paraformaldehyde, final concentration) were run periodically at saturating concentration and indicated no significant autohydrolysis of the substrate.

Preparation of DOM amendments

High-molecular weight DOM was isolated and concentrated from surface seawater as described in McCarren and colleagues (2010) with the following modifications. Four hundred thirty-four litres of surface seawater was obtained

using acid-cleaned Teflon tubing connected to a compressed air-driven diaphragm pump (Wilden, Grand Terrace, CA) and concentrated 100-fold over a period of 36 h using a single thin-film ultrafiltration membrane element (Separation Engineering, Escondido, CA, USA) in a custom-built polycarbonate membrane housing. Samples were taken for total organic carbon (TOC) quantification, cell counts and viral particle counts from the raw seawater, 0.2 μm filtrate and permeate water periodically during ultrafiltration and from the concentrate upon completion. This sample suite was also taken after serial filtration of the concentrate through a 0.1 μm Polycap TC prefilter (Whatman, GE Healthcare Life Sciences, Piscataway, NJ, USA) followed by a 30 kDa polyethersulfone membrane (Millipore) to remove viral particles as described in McCarren and colleagues (2010). Cell and viral counts determined pre- and post-30 kDa filtration using flow cytometry and fluorescence microscopy indicated the removal of cells, cell debris and the reduction of virus particles below ambient concentrations of seawater from the mixed layer at Station ALOHA (data not shown).

Prochlorococcus-derived DOM was isolated from an axenic culture of *Prochlorococcus* strain MIT9313 grown in 20 l of Pro99 medium prepared according to existing protocols (Moore *et al*., 2007) in sterile Sargasso seawater. The culture was maintained at 22°C and ca. 20 μmol photons m^{-2} s^{-1} and monitored for growth using bulk fluorescence. Upon reaching stationary phase, cell biomass was removed by centrifugation and 0.1 μm filtration (Whatman Polycap 36 TC capsule filter). Filtrate was acidified to pH 2–3 by adding trace metal grade hydrochloric acid before loading onto a custom packed column containing soxhlet purified octadecyl (C_{18}) functionalized silica gel (Sigma-Aldrich) at a rate of 2 ml min^{-1}. The column was then washed with ultrapure water (pH 2–3) at a flow rate of 1 ml min^{-1} to remove salts before eluting with 10 column volumes of acidified HPLC-grade methanol (pH 2–3) at a rate of 1 ml min^{-1}. Salt removal was confirmed using a silver nitrate solution, and the methanol elution was concentrated using a rotary evaporator. A subsample was taken for HPLC/MS analysis, and the remaining sample was dried using filtered high purity nitrogen gas, rinsed with ultrapure water to remove residual methanol and then dried again. Dried ProDOM material was stored in a combusted amber vial in the dark prior to resuspension at sea in filtered (0.1 μm Polycap TC; Whatman) seawater collected from 35 m at Station ALOHA.

Quantification of organic carbon and dissolved nitrogen

TOC and total dissolved nitrogen (TDN) were measured using the high temperature combustion method on a Shimadzu TOC-V_{CSH} with platinized aluminum catalyst coupled to a TNM-1 total nitrogen detector, while particulate organic carbon was measured at the University of California Davis Stable Isotope Facility. Details regarding sample handling and processing are provided in Supporting Information File S1.

Chromatographic separation and detection of MIT9313 metabolites

Chromatographic separation and detection of metabolites derived from *Prochlorococcus* strain MIT9313 was achieved using an Agilent 1200 series liquid chromatograph coupled to an Agilent 6130 mass spectrometer with an atmospheric ESI source. Mass spectral data were acquired from 100 to 2000 Da in the positive mode, and ions with minimum signal intensity fivefold greater than the maximum noise level were included in analysis. Details regarding run conditions and feature detection are provided in Supporting Information File S1.

Bioinformatics

Metagenomic and metatranscriptomic sequences derived from rRNA were identified using BLASTN with a bit score cut-off of 50 against a database composed of 5S, 16S, 18S, 23S and 28S rRNA sequences from microbial genomes and the SILVA LSU and SSU databases (http://www.arb-silva.de). Reads with best BLASTN hits to rRNA averaged 0.5% and 31% in DNA and cDNA libraries respectively, and these sequences were excluded from further analyses. Non-rRNA sequences with identical start sites (first 3 bp), 99% identity and ≤ 1 bp length difference were identified as probable artificially duplicated sequences (Stewart *et al*., 2010), which were removed using the cd-hit programme (Li and Godzik, 2006) and associated scripts (Gomez-Alvarez *et al*., 2009). Non-rRNA sequences were compared with the 31 May 2010 version of NCBI's nr protein reference database using BLASTX, and a bit score cut-off of 50 was used to identify significant matches. The MEGAN programme (Huson *et al*., 2007) was used to assign sequences to a higher-order taxonomy where sequences were assigned to the lowest common ancestor of a set of taxa if the bit scores of any database matches were within 3% of the top-scoring hit. The number of reads with significant matches to different taxonomic orders was normalized according to the total number of all significant hits to the NCBI-nr database for an individual sample.

To identify NCBI-nr reference genes with statistically significant read counts we used baySeq, a Bayesian method for identifying differential gene expression between samples (Hardcastle and Kelly, 2010). The DE of reference genes (posterior probability of ≥ 0.9) at the both the whole community and taxon-specific levels were determined between treatment and control metatranscriptomes for each time point individually (see Supporting Information File S1 for further details).

Using the method published in Ottesen and colleagues (2013), taxon-specific ortholog sequence clusters were generated separately for *Prochlorococcus*, *Pelagibacter* and the OM60 clade using sequenced genome representatives from NCBI. Within each taxon bin, transcript counts for genes shared between multiple reference genomes of the same taxa were combined into ortholog counts annotated with KEGG pathway information (see Supporting Information File S1 for further details). This approach was implemented to avoid artificial division of transcript pools from environmental organisms among multiple, imperfectly matched reference sequences (Ottesen *et al*., 2013). Analyses of transcriptional dynamics focused on changes in relative transcript abundance within each specific taxonomic bin. Significant DE of KEGG annotated orthologs (Datasets S2–S5) was used to direct and support comparisons of taxon-specific pathway

abundances through time. In some cases, nonsignificant orthologs are discussed in taxon-specific analyses as supporting information. Differentially expressed orthologs were further binned into central or auxiliary pathways (for specific details, see Supporting Information File S1). Heatmaps (Fig. 3) were generated in R using the heatmap.2 function in gplots (Warnes *et al*., 2009).

Acknowledgements

The authors would like to thank the cruise chief scientist S. Wilson and the captain and crew of the R/V *Ka'imikai-o-Kanaloa* for their help in collecting samples for this study. Our gratitude goes to R. Barry and T. Palden for all their hard work in preparing libraries for pyrosequencing and to J. Eppley for his great work on the DeLong lab sequencing pipeline. Many thanks to the Chisholm lab: P. Berube for providing spent *Prochlorococcus* medium for ProDOM extraction and A. Coe, J. Thompson and S. Roggensack for flow cytometry training. We thank C. Johnson for assistance with chromatographic and spectrometric data acquisition, M. Nieto-Cid for help with TOC/TDN analysis and J-H. Hehemann for the annotation of the OM60 GH and informative discussion. Thanks to L.A. Ventouras, C. Young, A. Martinez, F. Stewart and Y. Shi for valuable scientific discussions. This work is a contribution from the Center for Microbial Oceanography: Research and Education (C-MORE). This work was supported by a National Science Foundation Science and Technology Center Award EF0424599 (E.F.D and D.M.K.), grants to D.M.K., D.J.R and E.F.D from the Gordon and Betty Moore Foundation, a gift from the Agouron Institute (to E.F.D.) and a fellowship (202180) to A.K.S. from the Canadian Institutes of Health Research (CIHR).

References

Aluwihare, L.I., Repeta, D.J., and Chen, R.F. (1997) A major biopolymeric component to dissolved organic carbon in surface sea water. *Nature* **387:** 166–169.

Aluwihare, L.I., Repeta, D.J., and Chen, R.F. (1999) A comparison of the chemical characteristics of oceanic DOM and extracellular DOM produced by marine algae. *Mar Ecol Prog Ser* **186:** 105–117.

Aluwihare, L.I., Repeta, D.J., Pantoja, S., and Johnson, C.G. (2005) Two chemically distinct pools of organic nitrogen accumulate in the ocean. *Science* **308:** 1007–1010.

Azam, F. (1998) Microbial control of oceanic carbon flux: the plot thickens. *Science-New York Then Washington-* : 694–695.

Barra, L., Fontenelle, C., Ermel, G., Trautwetter, A., Walker, G.C., and Blanco, C. (2006) Interrelations between glycine betaine catabolism and methionine biosynthesis in *Sinorhizobium meliloti* strain 102F34. *J Bacteriol* **188:** 7195–7204.

Baumann, M.J., Eklöf, J.M., Michel, G., Kallas, M., Teeri, T.T., Czjzek, M., and Brumer, H. (2007) Structural evidence for the evolution of xyloglucanase activity from xyloglucan endo-transglycosylases: biological implications for cell wall metabolism. *Plant Cell Online* **19:** 1947–1963.

Bertlisson, S., Berglund, O., Pullin, M.J., and Chisholm, S.W. (2005) Release of dissolved organic matter by *Prochlorococcus*. *Vie Milieu* **55:** 225–232.

Carlson, C.A. (2002) Production and removal processes. In *Biogeochemistry of Marine Dissolved Organic Matter*. Hansell, D.A. (ed.). San Diego, CA, USA: Academic Press, pp. 91–152.

del Carmen Muñoz-Marín, M., Luque, I., Zubkov, M.V., Hill, P.G., Diez, J., and García-Fernández, J.M. (2013*) Prochlorococcus* can use the Pro1404 transporter to take up glucose at nanomolar concentrations in the Atlantic Ocean. *Proc Natl Acad Sci U S A* **110:** 8597–8602.

Cottrell, M.T., and Kirchman, D.L. (2000) Natural assemblages of marine proteobacteria and members of the Cytophaga-Flavobacter cluster consuming low- and high-molecular-weight dissolved organic matter. *Appl Environ Microbiol* **66:** 1692–1697.

Eilers, H., Pernthaler, J., and Amann, R. (2000) Succession of pelagic marine bacteria during enrichment: a close look at cultivation-induced shifts. *Appl Environ Microbiol* **66:** 4634–4640.

Field, C.B., Behrenfeld, M.J., Randerson, J.T., and Falkowski, P. (1998) Primary production of the biosphere: integrating terrestrial and oceanic components. *Science* **281:** 237–240.

Flärdh, K., Cohen, P.S., and Kjelleberg, S. (1992) Ribosomes exist in large excess over the apparent demand for protein synthesis during carbon starvation in marine Vibrio sp. strain CCUG 15956. *J Bacteriol* **174:** 6780–6788.

Frias-Lopez, J., Shi, Y., Tyson, G.W., Coleman, M.L., Schuster, S.C., Chisholm, S.W., and DeLong, E.F. (2008) Microbial community gene expression in ocean surface waters. *Proc Natl Acad Sci U S A* **105:** 3805–3810.

Fuhrman, J.A., Hewson, I., Schwalbach, M.S., Steele, J.A., Brown, M.V., and Naeem, S. (2006) Annually reoccurring bacterial communities are predictable from ocean conditions. *Proc Natl Acad Sci U S A* **103:** 13104–13109.

del Giorgio, P.A., and Duarte, C.M. (2002) Respiration in the open ocean. *Nature* **420:** 379–384.

Giovannoni, S.J., and Vergin, K.L. (2012) Seasonality in ocean microbial communities. *Science* **335:** 671–676.

Gomez-Alvarez, V., Teal, T.K., and Schmidt, T.M. (2009) Systematic artifacts in metagenomes from complex microbial communities. *ISME J* **3:** 1314–1317.

Gómez-Pereira, P.R., Hartmann, M., Grob, C., Tarran, G.A., Martin, A.P., Fuchs, B.M., *et al*. (2013) Comparable light stimulation of organic nutrient uptake by SAR11 and *Prochlorococcus* in the North Atlantic subtropical gyre. *ISME J* **7:** 603–614.

Hansell, D.A., Carlson, C.A., Repeta, D.J., and Schlitzer, R. (2009) Dissolved organic matter in the ocean: a controversy stimulates new insights.

Hardcastle, T.J., and Kelly, K.A. (2010) baySeq: empirical Bayesian methods for identifying differential expression in sequence count data. *BMC Bioinformatics* **11:** 422.

Hehemann, J.H., Correc, G., Barbeyron, T., Helbert, W., Czjzek, M., and Michel, G. (2010) Transfer of carbohydrate-active enzymes from marine bacteria to Japanese gut microbiota. *Nature* **464:** 908–912.

Huson, D.H., Auch, A.F., Qi, J., and Schuster, S.C. (2007) MEGAN analysis of metagenomic data. *Genome Res* **17:** 377–386.

Johnson, Z.I., Zinser, E.R., Coe, A., McNulty, N.P., Woodward, E.M., and Chisholm, S.W. (2006) Niche parti-

tioning among *Prochlorococcus* ecotypes along ocean-scale environmental gradients. *Science* **311:** 1737–1740.
Karl, D.M., and Lukas, R. (1996) The Hawaii Ocean Time-series (HOT) program: background, rationale and field implementation. *Deep Sea Res Part II Top Stud Oceanogr* **43:** 129–156.
Karl, D.M., Bidigare, R.R., Church, M.J., Dore, J.E., Letelier, R.M., Mahaffey, C., and Zehr, J. (2008) The nitrogen cycle in the North Pacific Trades biome: an evolving paradigm. *Nitrogen in the Marine Environment*: 705–769.
Karl, D.M., Church, M.J., Dore, J.E., Letelier, R.M., and Mahaffey, C. (2012) Predictable and efficient carbon sequestration in the North Pacific Ocean supported by symbiotic nitrogen fixation. *Proc Natl Acad Sci U S A* **109:** 1842–1849.
Kleber, H.P. (1997) Bacterial carnitine metabolism. *FEMS Microbiol Lett* **147:** 1–9.
Kujawinski, E.B., Longnecker, K., Blough, N.V., Vecchio, R.D., Finlay, L., Kitner, J.B., and Giovannoni, S.J. (2009) Identification of possible source markers in marine dissolved organic matter using ultrahigh resolution mass spectrometry. *Geochim Cosmochim Acta* **73:** 4384–4399.
Landa, M., Cottrell, M.T., Kirchman, D.L., Blain, S., and Obernosterer, I. (2013) Changes in bacterial diversity in response to dissolved organic matter supply in a continuous culture experiment. *Aquat Microb Ecol* **69:** 157–168.
Lauro, F.M., McDougald, D., Thomas, T., Williams, T.J., Egan, S., Rice, S., *et al*. (2009) The genomic basis of trophic strategy in marine bacteria. *Proc Natl Acad Sci U S A* **106:** 15527–15533.
Li, W., and Godzik, A. (2006) Cd-hit: a fast program for clustering and comparing large sets of protein or nucleotide sequences. *Bioinformatics* **22:** 1658–1659.
McCarren, J., Becker, J.W., Repeta, D.J., Shi, Y., Young, C.R., Malmstrom, R.R., *et al*. (2010) Microbial community transcriptomes reveal microbes and metabolic pathways associated with dissolved organic matter turnover in the sea. *Proc Natl Acad Sci U S A* **107:** 16420–16427.
Marie, D., Partensky, F., Jacquet, S., and Vaulot, D. (1997) Enumeration and cell cycle analysis of natural populations of marine picoplankton by flow cytometry using the nucleic acid stain SYBR green I. *Appl Environ Microbiol* **63:** 186–193.
Martínez, A., Osburne, M.S., Sharma, A.K., DeLong, E.F., and Chisholm, S.W. (2012) Phosphite utilization by the marine picocyanobacterium *Prochlorococcus* MIT9301. *Environ Microbiol* **14:** 1363–1377.
Martiny, A.C., Coleman, M.L., and Chisholm, S.W. (2006) Phosphate acquisition genes in *Prochlorococcus* ecotypes: evidence for genome-wide adaptation. *Proc Natl Acad Sci U S A* **103:** 12552–12557.
Martiny, A.C., Kathuria, S., and Berube, P.M. (2009) Widespread metabolic potential for nitrite and nitrate assimilation among *Prochlorococcus* ecotypes. *Proc Natl Acad Sci U S A* **106:** 10787–10792.
Mary, I., Garczarek, L., Tarran, G.A., Kolowrat, C., Terry, M.J., Scanlan, D.J., *et al*. (2008) Diel rhythmicity in amino acid uptake by Prochlorococcus. *Environ Microbiol* **10:** 2124–2131.
Michel, G., Chantalat, L., Duee, E., Barbeyron, T., Henrissat, B., Kloareg, B., and Dideberg, O. (2001) The kappa-carrageenase of *P. carrageenovora* features a tunnel-shaped active site: a novel insight in the evolution of Clan-B glycoside hydrolases. *Structure* **9:** 513–525.
Moore, L.R., Coe, A., Zinser, E.R., Saito, M.A., Sullivan, M.B., Lindell, D., *et al*. (2007) Culturing the marine cyanobacterium *Prochlorococcus*. *Limnol Oceanogr Methods* **5:** 353–362.
Mopper, K., Stubbins, A., Ritchie, J.D., Bialk, H.M., and Hatcher, P.G. (2007) Advanced instrumental approaches for characterization of marine dissolved organic matter: extraction techniques, mass spectrometry, and nuclear magnetic resonance spectroscopy. *Chem Rev* **107:** 419–442.
Muro-Pastor, M.I., Reyes, J.C., and Florencio, F.J. (2005) Ammonium assimilation in cyanobacteria. *Photosynth Res* **83:** 135–150.
Nelson, C.E., and Carlson, C.A. (2012) Tracking differential incorporation of dissolved organic carbon types among diverse lineages of Sargasso Sea bacterioplankton. *Environ Microbiol* **14:** 1500–1516.
Nissen, H. (1987) Long term starvation of a marine bacterium, *Alteromonas denitrificans*, isolated from a Norwegian fjord. *FEMS Microbiol Lett* **45:** 173–183.
Ottesen, E.A., Young, C.R., Eppley, J.M., Ryan, J.P., Chavez, F.P., Scholin, C.A., and Delong, E.F. (2013) Pattern and synchrony of gene expression among sympatric marine microbial populations. *Proc Natl Acad Sci U S A* **110:** E488–E497.
Partensky, F., Hess, W.R., and Vaulot, D. (1999) *Prochlorococcus*, a marine photosynthetic prokaryote of global significance. *Microbiol Mol Biol Rev* **63:** 106–127.
Poretsky, R.S., Sun, S., Mou, X., and Moran, M.A. (2010) Transporter genes expressed by coastal bacterioplankton in response to dissolved organic carbon. *Environ Microbiol* **12:** 616–627.
Rinta-Kanto, J.M., Sun, S., Sharma, S., Kiene, R.P., and Moran, M.A. (2012) Bacterial community transcription patterns during a marine phytoplankton bloom. *Environ Microbiol* **14:** 228–239.
Romera-Castillo, C., Sarmento, H., Alvarez-Salgado, X.A., Gasol, J.M., and Marrasé, C. (2011) Net production and consumption of fluorescent colored dissolved organic matter by natural bacterial assemblages growing on marine phytoplankton exudates. *Appl Environ Microbiol* **77:** 7490–7498.
Sarmento, H., and Gasol, J.M. (2012) Use of phytoplankton-derived dissolved organic carbon by different types of bacterioplankton. *Environ Microbiol* **14:** 2348–2360.
Sowell, S.M., Wilhelm, L.J., Norbeck, A.D., Lipton, M.S., Nicora, C.D., Barofsky, D.F., *et al*. (2009) Transport functions dominate the SAR11 metaproteome at low-nutrient extremes in the Sargasso Sea. *ISME J* **3:** 93–105.
Srinivasan, S., and Kjelleberg, S. (1998) Cycles of famine and feast: the starvation and outgrowth strategies of a marineVibrio. *J Biosci* **23:** 501–511.
Stewart, F.J., Ottesen, E.A., and DeLong, E.F. (2010) Development and quantitative analyses of a universal rRNA-subtraction protocol for microbial metatranscriptomics. *ISME J* **4:** 896–907.

Stingl, U., Tripp, H.J., and Giovannoni, S.J. (2007) Improvements of high-throughput culturing yielded novel SAR11 strains and other abundant marine bacteria from the Oregon coast and the Bermuda Atlantic Time Series study site. *ISME J* **1:** 361–371.

Sun, J., Steindler, L., Thrash, J.C., Halsey, K.H., Smith, D.P., Carter, A.E., *et al*. (2011) One carbon metabolism in SAR11 pelagic marine bacteria. *PLoS One* **6:** e23973.

Tada, Y., Taniguchi, A., Nagao, I., Miki, T., Uematsu, M., Tsuda, A., and Hamasaki, K. (2011) Differing growth responses of major phylogenetic groups of marine bacteria to natural phytoplankton blooms in the western North Pacific Ocean. *Appl Environ Microbiol* **77:** 4055–4065.

Teeling, H., Fuchs, B.M., Becher, D., Klockow, C., Gardebrecht, A., Bennke, C.M., *et al*. (2012) Substrate-controlled succession of marine bacterioplankton populations induced by a phytoplankton bloom. *Science* **336:** 608–611.

Tolonen, A.C., Aach, J., Lindell, D., Johnson, Z.I., Rector, T., Steen, R., *et al*. (2006) Global gene expression of *Prochlorococcus* ecotypes in response to changes in nitrogen availability. *Mol Syst Biol* **2:** 1–15.

Warnes, G.R., Bolker, B., and Lumley, T. (2009) gplots: various R programming tools for plotting data. *R package version 2*.

Yooseph, S., Nealson, K.H., Rusch, D.B., McCrow, J.P., Dupont, C.L., Kim, M., *et al*. (2010) Genomic and functional adaptation in surface ocean planktonic prokaryotes. *Nature* **468:** 60–66.

Zubkov, M.V., Fuchs, B.M., Tarran, G.A., Burkill, P.H., and Amann, R. (2003) High rate of uptake of organic nitrogen compounds by *Prochlorococcus* cyanobacteria as a key to their dominance in oligotrophic oceanic waters. *Appl Environ Microbiol* **69:** 1299–1304.

Zubkov, M.V., Tarran, G.A., and Fuchs, B.M. (2004) Depth related amino acid uptake by *Prochlorococcus* cyanobacteria in the Southern Atlantic tropical gyre. *FEMS Microbiol Ecol* **50:** 153–161.

Supporting Information

Additional Supporting Information may be found in the online version of this article at the publisher's web-site:

File S1. Includes supporting experimental procedures, Figure S1 and Tables S1–S12.
File S2. KEGG core and auxiliary pathway designations for *Prochlorococcus* and *Pelagibacter*.
Dataset S1. Taxon-specific ortholog cluster IDs, annotations, read counts and relative percentages for cDNA and DNA samples.
Dataset S2. *Prochlorococcus* differentially expressed KEGG orthologs organized by pathway for HMWDOM treatment versus Control.
Dataset S3. *Prochlorococcus* differentially expressed KEGG orthologs organized by pathway for ProDOM treatment versus Control.
Dataset S4. *Pelagibacter* differentially expressed KEGG orthologs organized by pathway for HMWDOM treatment versus Control.
Dataset S5. *Pelagibacter* differentially expressed KEGG orthologs organized by pathway for ProDOM treatment versus Control.
Fig. S1. Physiochemical characteristics of the mixed surface layer at Station ALOHA in 2010 plotted from the Hawaii Ocean Time-series Data Organization & Graphical System (HOT-DOGS) website (http://hahana.soest.hawaii.edu/hot/hot-dogs/) A) Monthly mixed layer depth calculated using potential temperature. B) Mean and standard deviation of monthly Low-level Nitrogen within the mixed layer depth. C) Mean and standard deviation of monthly Low-level Phosphate within the mixed layer depth. D) Mean and standard deviation of monthly Dissolved Organic Carbon within the mixed layer depth.
Table S1. Differentially expressed *Prochlorococcus* Orthologs enriched in HMWDOM belonging to auxiliary KEGG level 3 pathways.
Table S2. Differentially expressed *Prochlorococcus* Orthologs enriched in ProDOM belonging to auxiliary KEGG level 3 pathways.
Table S3. Differentially expressed *Pelagibacter* transport Orthologs underrepresented in HMWDOM.
Table S4. Differentially expressed *Pelagibacter* transport Orthologs underrepresented in ProDOM.
Table S5. Differentially expressed *Pelagibacter* transport Orthologs enriched in HMWDOM.
Table S6. Differentially expressed *Pelagibacter* transport Orthologs enriched in ProDOM.
Table S7. Differentially expressed *Pelagibacter* Orthologs enriched in HMWDOM belonging to auxiliary KEGG level 3 pathways.
Table S8. Differentially expressed *Pelagibacter* Orthologs enriched in ProDOM belonging to auxiliary KEGG level 3 pathways.
Table S9. Differentially expressed OM60 Orthologs enriched in HMWDOM.
Table S10. Differentially expressed OM60 Orthologs enriched in ProDOM.
Table S11. Differentially expressed OM60 Orthologs underrepresented in HMWDOM.
Table S12. Differentially expressed OM60 Orthologs underrepresented in ProDOM.